EVALUATION OF THE PHOTOCHEMICAL REFLECTANCE INDEX IN AVIRIS IMAGERY

John A. Gamon[1], Dar A. Roberts[2], and Robert O. Green[3]

[1]Department of Biology & Microbiology
California State University, Los Angeles
5151 State University Drive
Los Angeles, CA 90032

[2]Department of Geography
University of California, Santa Barbara
Santa Barbara, CA 93106

[3]Jet Propulsion Laboratory
California Institute of Technology
4800 Oak Grove Drive
Pasadena, CA 91109

1. INTRODUCTION

In this paper, we evaluate the potential for extracting the "photochemical reflectance index" (PRI; previously called the "physiological reflectance index") from AVIRIS data. This index, which is derived from narrow-band reflectance at 531 and 570 nm, has proven to be a useful indicator of photosynthetic function at the leaf and canopy scales (Gamon and Field 1992, Gamon et al. 1992, Peñuelas et al. *in review*).

At the leaf level, PRI varies with photosynthetic capacity, radiation-use efficiency, and vegetation type (unpublished data). This finding is consistent with the hypothesis that vegetation types exhibiting chronically reduced photosynthesis during periods of stress (e.g. drought-tolerant evergreens) invest proportionally more in photoprotective processes than vegetation with high photosynthetic capacity (e.g. crops or deciduous perennials).

Vertical transects in tropical and boreal forest canopies have indicated declines in PRI associated with downregulation of photosynthesis at the canopy tops under sunny, dry midday conditions (unpublished data). This reduced PRI in upper canopy levels provides a further basis for examining this signal with the "view from above" afforded by aircraft overflights.

Although many factors could confound interpretation of a subtle physiological signal at the landscape scale, we conducted a preliminary examination of PRI extracted from existing AVIRIS imagery of Stanford University's Jasper Ridge Biological Preserve obtained on the June 2nd, 1992, overflight. The goal was to use the hyperspectral capabilities of AVIRIS to evaluate the potential of this index for obtaining useful physiological data at the landscape scale. The expectation based on leaf- and canopy-level studies was that regions containing vegetation of reduced photosynthetic capacity (e.g. chaparral or evergreen woodland) would exhibit lower PRI values than regions of high capacity (e.g. deciduous woodland).

2. METHODS

In this study, PRI was calculated as follows:

$$PRI = (R_{528}-R_{567})/(R_{528}+R_{567}) \qquad (1)$$

Where R_{528} and R_{567} indicate reflectance at AVIRIS bands 15 (528 nm) and 19 (567 nm), respectively. These represent the AVIRIS bands closest to 531 and 570 nm, which are typically used for this index.

The Normalized Difference Vegetation Index (NDVI), a widely used canopy greenness indicator, was calculated as:

$$NDVI = (R_{831} - R_{667})/(R_{831} + R_{667}) \qquad (2)$$

Where R_{831} and R_{667} indicate reflectance at AVIRIS bands 49 (831 nm) and 29 (667 nm), respectively. A portion of an AVIRIS spectrum for the deciduous woodland is illustrated in Figure 1, along with the bands used for calculating PRI and NDVI.

Reflectance images were derived using the approach described by Green et al. (1993a &b). This approach uses MODTRAN II radiative transfer code to generate a series of look-up tables for an AVIRIS scene collected at a specific latitude and longitude on a specific date. Look-up tables are generated for a black target and for a 25% reflective target. Radiance estimated for the black target provides an estimate of the additive path radiance. For this analysis aerosol optical depth was estimated and assumed to be constant across the scene. Once the look-up tables are generated a non-linear least squares fitting routine is employed to invert radiance measured at the sensor and solve for atmospheric column water vapor abundance and liquid water absorption. This approach is applied to each element in the scene to produce images showing liquid water and water vapor abundance. Once atmospheric column water vapor abundance has been determined for a specific element, reflectance can be retrieved using the general equation:

$$R_{ij\lambda} = 0.25 \times (L_{ij\lambda} - L_{\lambda_p'}) / (L_{\lambda'} - L_{\lambda_p'}) \qquad (3)$$

Where $R_{ij\lambda}$ indicates reflectance at sample i, line j, and wavelength λ; $L_{ij\lambda}$ is the measured radiance at the sensor; $L_{\lambda_p'}$ is the modeled path radiance; and $L_{\lambda'}$ is the modeled radiance at the sensor for a 25% reflective target (at an estimated water vapor abundance). For this analysis water vapor was estimated from the 940 nm water vapor band.

3. RESULTS & DISCUSSION

As predicted, the PRI values from the Jasper Ridge AVIRIS scene were lower in vegetation with reduced photosynthetic capacity (e.g. chaparral and evergreen woodland) than in the high-capacity vegetation (deciduous woodland). The two grassland types, which were largely comprised of senescent vegetation by this date, had the lowest PRI values (Figure 2). These results were consistent with the hypothesis (based on prior, leaf-level studies) that PRI scales with photosynthetic capacity and radiation-use efficiency in a wide variety of species.

In addition to photosynthetic function, many other factors (including canopy structure, phenology, and atmospheric effects) could explain the PRI patterns in Jasper Ridge imagery. PRI varied with canopy "greenness" (measured by NDVI; Figure 2), suggesting that PRI was strongly influenced by canopy structure and phenology at the landscape scale. Clearly, the spectral region (AVIRIS bands 15 and 19) used for PRI calculation presents technical challenges to a simple interpretation of this index in landscape imagery. Until these confounding issues are resolved, PRI appears to be more directly applicable to laboratory and ground-based field studies than to landscape-level remote sensing.

Further research will clarify the relative influence of photosynthetic regulation, canopy structure and phenology, atmospheric effects, and other factors on PRI. Approaches for resolving these issues might include mixture modeling or other image classification methods. Application of canopy radiative transfer models could also be of use. Further field experiments combining ground optical sampling (e.g. using access towers) with CO_2 flux measurements (e.g. eddy covariance) are also warranted. Our current plans are to address some of these remaining issues using AVIRIS imagery and other measurements obtained from recent Jasper Ridge and boreal forest overflights.

4. REFERENCES

Gamon, J.A. and Field, C.B. (1992) Tracking photosynthetic efficiency with narrow-band spectroradiometry. *Summaries of the Third Annual JPL Airborne Geoscience Workshop,* Vol. 1, JPL Pub. 92-14, Jet Propulsion Laboratory, Pasadena, CA, June 1992, pp. 95–97.

Gamon, J.A., Peñuelas, J., and Field, C.B. (1992) A narrow-waveband spectral index that tracks diurnal changes in photosynthetic efficiency. *Remote Sensing of Environment.* Vol. 41, pp. 35–44.

Green, R.O., Conel, J.E., and Roberts, D.A., 1993a, Estimation of aerosol optical depth pressure elevation, water vapor and calculation of apparent surface reflectance from radiance measured by the Airborne Visible-Infrared Imaging Spectrometer (AVIRIS) using MODTRAN2, SPIE Conference Vol. 1937 (Imaging Spectrometry of the Terrestrial Environment), pp. 2–11.

Green, R.O., Conel, J.E., and Roberts, D.A., 1993b, Estimation of aerosol optical depth and additional atmospheric parameters for the calculation of apparent reflectance from radiance measured by the Airborne Visible/Infrared Imaging Spectrometer, Summaries of the 4th Annual JPL Airborne Geoscience Workshop, Oct. 25–29, 1993, Washington, D.C., JPL Pub. 93-26, Jet Propulsion Lab, Pasadena, CA, Vol. 1. AVIRIS Workshop, pp. 73–76.

Peñuelas, J., Filella, I., and Gamon, J.A.. (in review) Assessment of photosynthetic radiation-use efficiency with spectral reflectance, *Plant, Cell and Environment.*
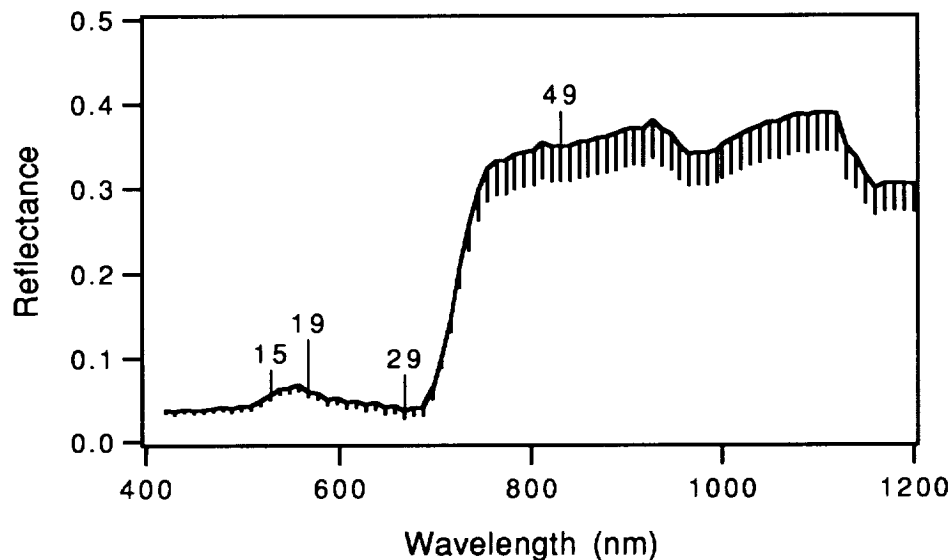
Figure 1. Representative AVIRIS spectrum (average of 10 pixels) for a deciduous woodland at Jasper Ridge. The AVIRIS bands used for calculating PRI (bands 15 and 19) and NDVI (bands 29 and 49) are indicated. Error bars indicate 1 standard error of the mean (SEM).
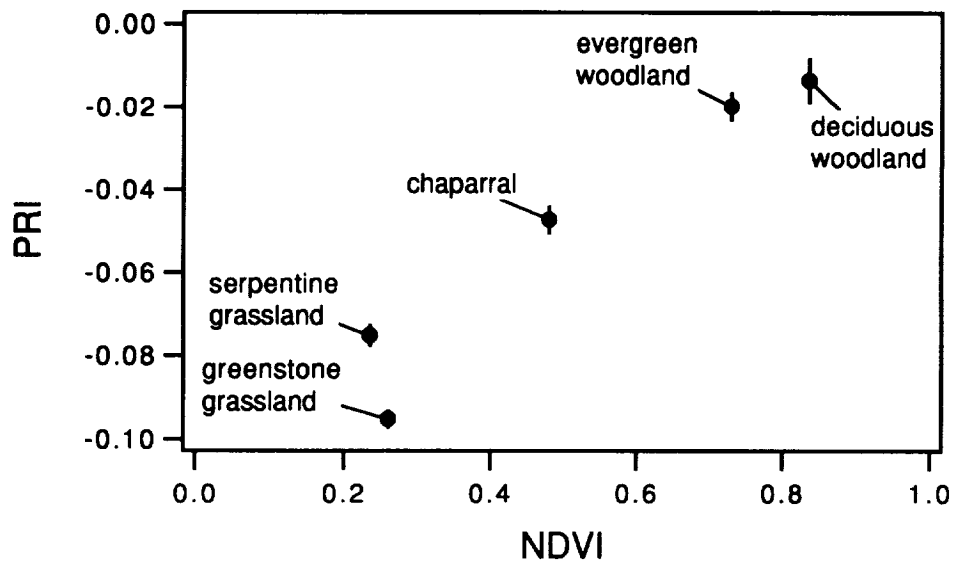
Figure 2. Comparison of PRI with NDVI values for five vegetation types at Jasper Ridge. Each point represents the mean ($\pm$ 1 SEM) for 10 pixels. As predicted from leaf-level studies (not shown), PRI increases with photosynthetic capacity and radiation-use efficiency, with woodland vegetation exhibiting relatively high capacity and efficiency compared to chaparral or grassland. However, the correlation of PRI with NDVI suggests that the relationship between PRI and photosynthetic function is largely driven by green canopy structure in this AVIRIS image.

5. ACKNOWLEDGMENT